De Falco, P. E., Watkins, G., Mimis, K., Bensmida, S., & Morris, K. (2019). Analysis of optimal outphasing load trajectories for GaN Pas. In *2018 Asia-Pacific Microwave Conference, APMC 2018 - Proceedings* (Vol. 2018-November, pp. 58-60). [8617660] Institute of Electrical and Electronics Engineers (IEEE). https://doi.org/10.23919/APMC.2018.8617660

Analysis of Optimal Outphasing Load Trajectories for GaN PAs

Paolo Enrico de Falco, Gavin Watkins
Toshiba Research Europe Ltd.
Telecommunication Research Lab
Bristol, United Kingdom

Konstantinos Mimis, Souheil Bensmida, Kevin Morris
University of Bristol
Communication Systems and Network Lab
Bristol, United Kingdom

***Abstract*—This paper presents an analysis of the optimal Z_{f_0} load trajectories of saturated GaN PAs through Z_{f_0} and Z_{2f_0} load-pull measurements under constant input power on a 900 MHz 10 W PA. It is shown that a DE >50% at 10 dB back-off can be obtained for a range of 160° of $\angle Z_{2f_0}$ when Z_{f_0} is set to its optimal point. The black box combiner design equations are used as a tool to determine the complete outphasing load trajectories for outphasing systems designed for different back-off levels and extract drain efficiency performance for a range of $\angle Z_{2f_0}$ terminations. When the suboptimal outphasing load trajectories are considered, Z_{2f_0} is demonstrated to have a greater impact compared to the case Z_{f_0} follows the optimal load trajectories.**

***Index Terms*—outphasing, harmonically tuned PAs**

I. Introduction

In modern high data-rate wireless communication systems, strict requirements are set for the RF power amplifier (PA) due to the need to transmit RF signals with large peak-to-average power ratios (PAPR) and the need to operate the transmitter at different average power levels. For the RF designer, this translates into maintaining a high PA drain efficiency (DE) over a large P_{OUT} dynamic range. At the same time it is critical to maximise the gain of the PA and achieve the largest saturated P_{OUT} for a given device. Load modulated architectures such as Doherty [1] and outphasing [2] are powerful ways this can be achieved. Fig. 1 (a) shows the potential for efficiency enhancement of a load modulated architecture over 12 dB P_{OUT} from Z_{f_0} and Z_{2f_0} load-pull of a 900 MHz GaN PA under constant input power. The dependency of back-off efficiency of GaN PAs on Z_{2f_0} was analysed in [3] with simulations and experiments considering PAs operating at fixed compression (1 dB). In order to achieve the largest possible back-off efficiency load modulated architectures, such as outphasing, operate the constituent branch PAs at much larger compression levels, pushing the device to exhibit switch-like behaviour. Fig. 1 (b) shows that even operating in deep saturation as the PA is driven with constant input power, the optimal $\angle\Gamma_{2f_0}$ for DE of a single-ended GaN PA increases from 50° to 250°. The aim of this experiment is to investigate the optimal Z_{f_0} load trajectories of a highly saturated GaN PA for different Z_{2f_0} terminations. Extensive load-pull measurements are presented for a 900 MHz GaN HEMT single-ended PA, which are de-embedded to the current generator (CG) plane of the device. The optimal Z_{f_0} load trajectories for fixed Z_{2f_0} terminations are compared to the real loading condition achievable with outphasing operation, for different output power back-off (OPBO) levels.

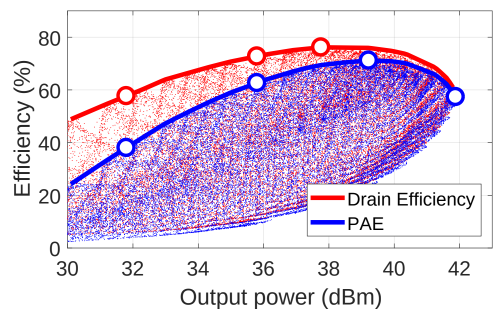

(a)

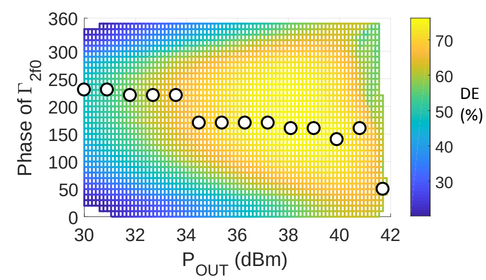

(b)

Fig. 1: Performance of PA subject to Z_{f_0} and Z_{2f_0} load-pull (a) and variation in optimal Z_{2f_0} over P_{OUT} (b).

II. Experiment Overview and Set-Up

Fig. 2 (a) shows a block diagram of the experiment set-up and measurements of the pre-matching network. The single-ended PA was designed using a 10 W GaN device with 0.76 mm Duroid 5880 substrate. The PA, which is shown in Fig. 2 (b), is pre-matched at the output for DE at Z_{f_0} only with a high-pass lumped LC network. The PA was biased in class-B ($V_{\mathrm{GS}} = -3V$ and $V_{\mathrm{DS}} = 28V$). Throughout the measurements the source tuner presented to the input of the PA a fixed conjugate match impedance while the output third harmonic Γ_{3f_0} was set for maximum DE at saturation and also fixed. The PA, fed with a pulsed single-tone at a constant power level (27dBm), was load-pulled at Z_{f_0} for 72 values of Γ_{2f_0} corresponding to $|\Gamma_{2f_0}| = 0.92$, the $|\Gamma|$ limit of the set-up, and with $\angle\Gamma_{2f_0}$ swept from 0° to 360° with 5° resolution. The matching network, connectors, intrinsic and extrinsic device parasitic s-parameters were cascaded and used so to be able to de-embed the impedances presented during load-pull by the

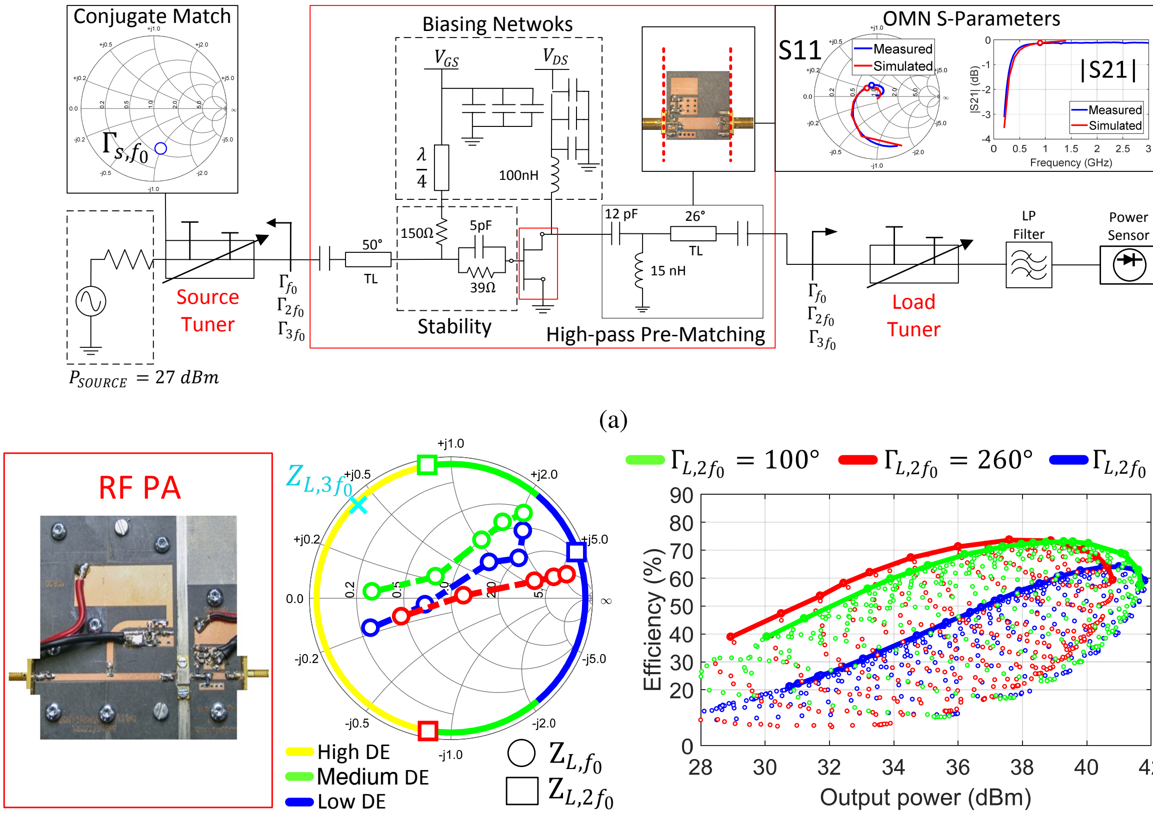

(a)

(b) (c) (d)

Fig. 2: Set-up block diagram (a), photograph of RF PA (b), optimal load trajectories for different $Z_{2\mathrm{f}_0}$ (c) and DE vs P_{OUT} performance (d).

load tuner, calibrated to the output of the PA, to its CG plane.

III. Optimal Load Trajectories with fixed $Z_{2\mathrm{f}_0}$

The optimal load trajectories and respective performance, for three different $\angle\Gamma_{2\mathrm{f}_0} = [20°; 100°; 260°]$ corresponding respectively to a short, a capacitive reactive and inductive reactive impedance, after de-embedding to the CG plane of the device, are shown in Fig. 2 (c). The optimal Z_{f_0} trajectories with a fixed Z_{2f_0} are defined as the load trajectories which, starting from the maximum P_{OUT} point, $Z_{\mathrm{f}_0,\mathrm{p}}$, pass through the optimal DE point $Z_{\mathrm{f}_0,\eta}$ and follow the convex hull of the DE vs P_{OUT} profile, resulting from Z_{f_0} load-pull. The first finding evident from Fig. 2 (c) and (d) is that, following the optimal Z_{f_0} load trajectory with a fixed $Z_{2\mathrm{f}_0}$, a DE $> 50\%$ at 10 dB OPBO can be maintained for a range of 160° of Γ_{2f_0}. Additionally, it is noted that an even larger region of efficiency exists as DE $> 40\%$ at 10 dB OPBO over 260° Γ_{2f_0}. As Γ_{2f_0} approaches a intrinsic CG short, DE at OPBO progressively degrades, and the DE vs P_{OUT} profile changes substantially as evidenced in Fig. 2 (d). Although in the high efficiency region DE at 10 dB OPBO presents small variation, a degradation of 1 dB in P_{OUT} is evident moving from $\Gamma_{2f_0} = 100°$ to $\Gamma_{2f_0} = 260°$. The continuity of modes of operation [4] is a well-known concept in the PA design community and reflects the possibility of obtaining quasi-identical P_{OUT} for a range of different $Z_{2\mathrm{f}_0}$ conditions. This concept was expanded to PAs in switch-mode operation [5]. The results presented in this paper show that through a continuum of switch-mode of operation conditions, which correspond to the Γ_{2f_0} high efficiency region in Fig. 2 (c), high DE can be achieved over a 10 dB P_{OUT} dynamic range, once the PA is highly saturated. As the input power is fixed during load-pull, performance in terms of DE is shown to demonstrate a measure of waveform shape integrity; however it is expected that with mixed-mode approach PAE could be restored by improving the system gain.

IV. Outphasing Load Trajectories

When Z_{f_0} follows the optimal load trajectories, the DE can be kept high over a large dynamic range with a fixed $Z_{2\mathrm{f}_0}$. However, during outphasing operation the two branch PAs are loaded identically only at two outphasing angles which correspond to the intersection of their load modulation trajectories: at the peak power point, and the chosen OPBO point. At these points performance can be ensured when designing from load-pull and using the optimal load trajectory for the chosen $Z_{2\mathrm{f}_0}$. However, no information is known on the performance of the system throughout the rest of outphasing operation. It is possible to extract the performance of the outphasing PA for a chosen $Z_{2\mathrm{f}_0}$ and OPBO, using $Z_{\mathrm{f}_0,\mathrm{p}}$ and $Z_{\mathrm{f}_0,\eta,\mathrm{OPBO}}$ with the black box combiner design equations [1]:

$$Z_{11} = \frac{Z_{\mathrm{f}_0,\eta,\mathrm{OPBO}} - Z_{\mathrm{f}_0,\mathrm{p}}}{1 + e^{j2\theta_1}} + Z_{\mathrm{f}_0,\mathrm{p}} \quad (1)$$

$$Z_{12} = \frac{1}{2}(Z_{\mathrm{f}_0,\mathrm{p}} - Z_{\mathrm{f}_0,\eta,\mathrm{OPBO}})\sec(\theta_1) \quad (2)$$

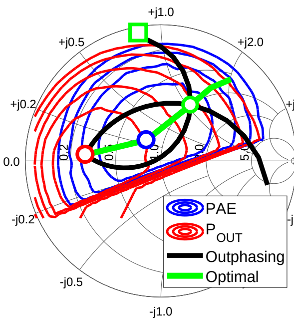

(a)

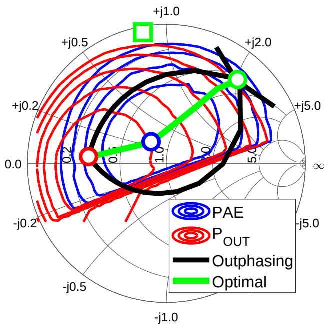

(b)

Fig. 3: P_{OUT} and PAE load-pull contours, optimal $Z_{\mathrm{f_0}}$ and outphasing load trajectories optimised for 6 and 10 dB OPBO.

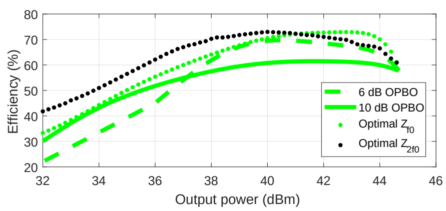

(a)

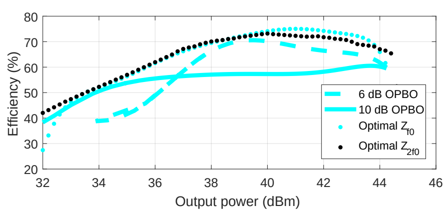

(b)

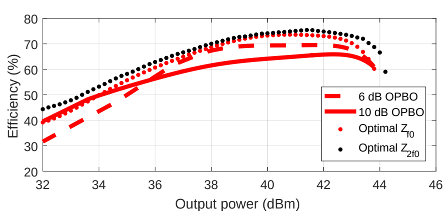

(c)

Fig. 4: DE vs P_{OUT} for different outphasing load trajectories for $\Gamma_{2\mathrm{f_0}} = 100°$ (a), $\Gamma_{2\mathrm{f_0}} = 180°$ (b), $\Gamma_{2\mathrm{f_0}} = 260°$ (c).

$$Z_{22} = \frac{Z_{\mathrm{f_0,p}} - Z_{\mathrm{f_0},\eta,\mathrm{OPBO}}}{1 + e^{j2\theta_1}} + Z_{\mathrm{f_0},\eta,\mathrm{OPBO}} \tag{3}$$

The complete outphasing load trajectories are determined by approximating the PA branches as voltage sources with the two-port combiner found from (1)-(3). The outphasing trajectories and performance are extracted for an outphasing system designed for: OPBO = 6 and 10 dB. The performance of the upper branch PA only is extracted for simplicity to calculate an approximate system DE. Three $\Gamma_{2\mathrm{f_0}}$ are considered, chosen from the high efficiency region found in Section III. The outphasing load trajectories considered for $\angle\Gamma_{2\mathrm{f_0}} = 100°$ are shown in Fig. 3. The outphasing performance is compared to the performance of the optimal $Z_{\mathrm{f_0}}$ load trajectory with fixed $Z_{2\mathrm{f_0}}$ and to that of an outphasing system with a dynamic

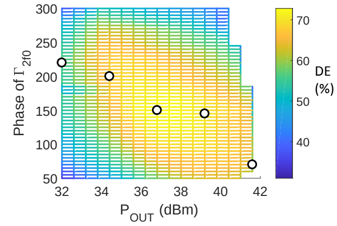

(a)

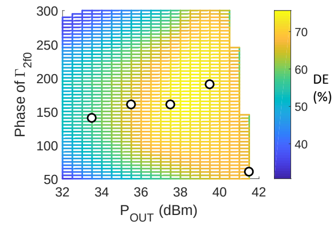

(b)

Fig. 5: Variation of optimal $\angle\Gamma_{2f_0}$ for 6 dB outphasing upper and lower branch trajectories optimised for $\angle\Gamma_{2\mathrm{f_0}} = 100°$.

optimal $Z_{2\mathrm{f_0}}$ at each point of its trajectories, as shown in Fig. 4. As expected the trajectories optimised for 6 dB OPBO present a DE closer to the optimal $Z_{\mathrm{f_0}}$ case at small OPBO levels, with the DE quickly dropping off at larger OPBO. Conversely, when optimised for 10 dB OPBO, the efficiency of the system is lower at smaller P_{OUT}, due to the greater deviation of the load trajectories from the optimal $Z_{\mathrm{f_0}}$. The performance of the outphasing system with optimised $Z_{2\mathrm{f_0}}$ outperforms all other cases. Tuning of $Z_{2\mathrm{f_0}}$ restores the maximum P_{OUT} capability of the device for each case considered. In Fig. 5 the region of optimal DE for upper and lower branch outphasing trajectories are shown. Due to the shape of the outphasing trajectories, the $Z_{2\mathrm{f_0}}$ high efficiency region shifts with the optimal $Z_{2\mathrm{f_0}}$ for the upper and lower branches following opposite trends.

V. Conclusion

This paper has presented $Z_{\mathrm{f_0}}$ and $Z_{2\mathrm{f_0}}$ load-pull measurements on a 900 MHz 10 W GaN HEMT single-ended PA presenting and comparing the optimal load trajectories over output power, with fixed $Z_{2\mathrm{f_0}}$. A wide $Z_{2\mathrm{f_0}}$ high efficiency region corresponding to large inductive and capacitive intrinsic loading is demonstrated. A simple way to extract outphasing performance from load-pull contours using the black box design equations is shown and used to demonstrate the significance of $Z_{2\mathrm{f_0}}$ tuning when the PA is presented with real suboptimal outphasing trajectories.

References

[1] M. Özen, K. Andersson and C. Fager, “Symmetrical Doherty Power Amplifier With Extended Efficiency Range,” in *IEEE Trans. on Microw. Theory and Techn.*, vol. 64, no. 4, pp. 1273-1284, April 2016.

[2] M. Pampn-Gonzlez et all, “Outphasing combiner synthesis from transistor load pull data,” in *IEEE MTT-S Int. Microw. Symp. Dig*, Jun. 2015, pp. 1-4.

[3] P.E. de Falco et all, “Load Modulation of Harmonically Tuned Amplifiers and Application to Outphasing Systems,” in *IEEE Trans. Microw. Theory and Techn.*, vol. 65, no. 10, pp. 3596-3612, Oct. 2017.

[4] S. C. Cripps, P. J. Tasker, A. L. Clarke, J. Lees and J. Benedikt, “On the Continuity of High Efficiency Modes in Linear RF Power Amplifiers,” in *IEEE Microw. Wireless Compon. Lett.*, vol. 19, no. 10, pp. 665-667, Oct. 2009.

[5] M. Özen, R. Jos and C. Fager, “Continuous Class-E Power Amplifier Modes,” in *IEEE Transactions on Circuits and Systems II: Express Briefs*, vol. 59, no. 11, pp. 731-735, Nov. 2012.